

# Synthesis of CdSeS Nanocrystals in Coordinating and Noncoordinating Solvents: Solvent's Role in Evolution of the Optical and Structural Properties

Najeh Al-Salim,<sup>\*,†</sup> Aidan G. Young,<sup>‡</sup> Richard D. Tilley,<sup>§</sup> A. James McQuillan,<sup>‡</sup> and James Xia<sup>†</sup>

Industrial Research, Ltd., P.O. Box 31-310, Lower Hutt, New Zealand, Chemistry Department, University of Otago, P.O. Box 56, Dunedin, New Zealand, and McDiarmid Institute for Advanced Materials and Nanotechnology, Victoria University of Wellington, P.O. Box 600, Wellington, New Zealand

Received March 26, 2007. Revised Manuscript Received July 26, 2007

CdSe<sub>x</sub>S<sub>y</sub> nanocrystals were synthesized in eight solvents that have different coordinating properties, trioctylphosphine oxide, trioctylphosphine, triphenylphosphine, oleylamine, hexadecylamine, dioctylamine, triethylamine, and 1-octadecene at 230–300 °C. These nanocrystals exhibited high photoluminescence, which could be tuned over most of the visible region by changing the Se/S ratio or the solvent. The nanocrystals were characterized using UV–vis and IR spectroscopy, TEM, EDS, XRD, and NMR. <sup>31</sup>P NMR and IR studies provided vital information about the nanocrystal surface capping ligands, indicating that those prepared in noncoordinating solvents were stabilized in solution mainly by oleic acid while those prepared in the coordinating solvents were stabilized mainly by solvent, phosphine and phosphine sulfide ligands, and some oleic acid. The hexagonal or cubic phase of these nanocrystals can be selectively prepared at temperatures as high as 300 °C by choosing the appropriate solvent.

## Introduction

Recent advances in nanotechnology have offered new approaches for the synthesis of semiconductor nanomaterials, which have electronic properties intermediate between those of the bulk and the molecular states. II–VI metal chalcogenide nanocrystals (also known as quantum dots, QDs) such as CdS,<sup>1</sup> CdSe<sup>2</sup> and CdTe<sup>3</sup> have been shown to exhibit efficient photoluminescence (PL) due to quantum confinement<sup>4</sup> in the small nanocrystals. The PL spectra of these QDs can be tuned over a wide range of the spectrum depending on their size and composition.<sup>1–3</sup> QDs have many advantages over organic dyes, such as high PL with narrow and symmetric emission spectra and higher stability against photobleaching.<sup>5</sup> They also show a unique property in that a single wavelength of light can excite all colors of QDs. Due to these excellent properties, these nanocrystals are

becoming promising tools in biotechnology and medical applications, as ultrasensitive fluorescent probes<sup>6</sup> and in optoelectronic devices,<sup>7</sup> and have potential use in near-IR communication devices.<sup>8</sup>

In order to increase the PL quantum yield (QY) and the photostability of bare CdSe nanocrystals by a few times, a thin layer of material with lattice parameters similar to that of CdSe and with a higher band gap can be grown on the core (core/shell) leading to charge carrier confinement and significant enhancement of the quantum yield, e.g., core/shell CdSe/ZnS<sup>10–13,25</sup> and CdSe/CdS.<sup>14–16</sup> However, core/

\* Corresponding author. E-mail: n.al-salim@irl.cri.nz.

<sup>†</sup> Industrial Research, Ltd.

<sup>‡</sup> University of Otago.

<sup>§</sup> Victoria University of Wellington.

- (1) (a) Zhang, Z. H.; Chin, W. S.; Vittal, J. J. *J. Phys. Chem. B* **2004**, *108*, 18569. (b) Pan, D.; Jiang, S.; An, L.; Jiang, B. *Adv. Mater.* **2004**, *16*, 982. (c) Lazell, M.; O'Brien, P. J. *Mater. Chem.* **1999**, *9*, 1381. (d) Yu, W. W.; Peng, X. *Angew. Chem., Int. Ed.* **2002**, *41*, 2368.
- (2) (a) Peng, Z. A.; Peng, X. *J. Am. Chem. Soc.* **2001**, *123*, 183. (b) Qu, L.; Peng, X. *J. Am. Chem. Soc.* **2002**, *124*, 2094. (c) Dabbousi, B. O.; Rodriguez-Viejo, J.; Mikulec, F. V.; Heine, J. R.; Mattoussi, H.; Ober, R.; Jensen, K. F.; Bawendi, M. G. *J. Phys. Chem. B* **1997**, *101*, 9463. (d) Peng, Z. A.; Peng, X. *J. Am. Chem. Soc.* **2002**, *124*, 3343.
- (3) (a) Li, L.; Qian, H.; Ren, J. *Chem. Commun.* **2005**, 528. (b) Gao, M.; Kirstein, S.; Möhwald, H.; Rogach, A. L.; Kornowski, A.; Eychmüller, A.; Weller, H. *J. Phys. Chem. B* **1998**, *102*, 8360. (c) Bao, H.; Gong, Y.; Li, Z.; Gao, M. *Chem. Mater.* **2004**, *16*, 3853. (d) Zheng, Y.; Gao, S.; Ying, J. Y. *Adv. Mater.* **2007**, *19*, 376. (e) Nakashima, T.; Kawai, T. *Chem. Commun.* **2005**, 1643.
- (4) Brus, L. E. *J. Chem. Phys.* **1986**, *90*, 2555.
- (5) Chan, W. C. W.; Nie, S. *Science* **1998**, *281*, 2016.

- (6) (a) Bruchez, M., Jr.; Moronne, M.; Gin, P.; Weiss, S.; Alivisatos, A. P. *Science* **1998**, *281*, 2013. (b) Goldman, E. T.; Balighian, E. D.; Mattoussi, H.; Kuno, M. K.; Mauro, J. M.; Tran, P. T.; Anderson, G. P. *J. Am. Chem. Soc.* **2002**, *124*, 6378. (c) Jaiswal, J. K.; Goldman, E. R.; Mattoussi, H.; Simon, S. M. *Nat. Methods* **2004**, *1*, 73. (d) Michalet, X.; Pinaud, F. F.; Entolila, L. A.; Tsay, J. M.; Doose, S.; Li, J. J.; Sundaresan, G.; Wu, A. M.; Gambhir, S. S.; Weiss, S. *Science* **2005**, *307*, 538. (e) So, M.-K.; Xu, C.; Loening, A. M.; Gambhir, S. S.; Rao, J. *Nat. Mater.* **2006**, *24*, 339.
- (7) (a) Lee, J.; Sundar, V. C.; Heine, J. R.; Bawendi, M. G.; Jensen, K. F. *Adv. Mater.* **2000**, *12*, 1102. (b) Guldi, D. M.; Zilbermann, I.; Anderson, G.; Kotov, N. A.; Tagmatarchis, N.; Prato, M. *J. Mater. Chem.* **2005**, *15*, 114. (c) Zhao, J.; Bardecker, J. A.; Munro, A. M.; Liu, M. S.; Niu, Y.; Ding, I.-K.; Luo, J.; Chen, B.; Jen, A. K.-Y.; Ginger, D. S. *Nano Lett.* **2006**, *6*, 463.
- (8) (a) Kershaw, S. V.; Burt, M.; Ahrrison, M.; Togach, A.; Weller, H.; Eychmüller, A. *Appl. Phys. Lett.* **1999**, *75*, 1694. (b) Schaller, R. D.; Petruska, M. A.; Klimov, V. K. *J. Phys. Chem. B* **2003**, *107*, 13765. (c) Sargent, E. H. *Adv. Mater.* **2005**, *17*, 515.
- (9) (a) Murray, C. B.; Norris, D. J.; Bawendi, M. G. *J. Am. Chem. Soc.* **1993**, *115*, 8706. (b) Steigerwald, M. L.; Alivisatos, A. P.; Gibson, J. M.; Harris, T. D.; Kortan, R.; Muller, A. J.; Thayer, A. M.; Duncan, T. M.; Douglass, D. C.; Brus, L. E. *J. Am. Chem. Soc.* **1988**, *110*, 3046.
- (10) Bullen, C.; Mulvaney, P. *Langmuir* **2006**, *22*, 3007.
- (11) Hines, M. A.; Guyot-Sionnest, P. *J. Phys. Chem.* **1996**, *100*, 468.
- (12) Talapin, D. V.; Rogach, A. L.; Kornowski, A.; Haase, M.; Weller, H. *Nano Lett.* **2001**, *1*, 207.

shell fabrication may add more complication to the synthesis method, which limits large-scale preparation.

Research in alloyed bichalcogenide nanocrystals of type  $\text{ME}_x\text{E}'_y$  ( $\text{M}$  = metal,  $\text{E}$  and  $\text{E}'$  = different chalcogen atoms,  $x + y \approx 1$ ) such as  $\text{ZnSeS}$ ,  $\text{CdSeS}$ , and  $\text{CdSeTe}$ <sup>17–20</sup> appears to be very limited, but it offers an alternative one-step synthesis to create QDs with tuneable photoluminescence through the visible range by varying the alloy composition. One-step synthesis of alloyed chalcogenides has the benefit of omitting the step of nanocrystals shell coating which is required for some metal chalcogenides to improve their photoluminescence. The other advantage of the  $\text{CdSeS}$  system over the core/shell system is the possibility of forming a series of nanocrystals that have different PL wavelengths with high quantum yield but are very close in size. This may be achieved by carefully changing the chalcogen composition in the nanocrystals rather than the size to tune the absorption and emission properties. The factors that affect the formation of bichalcogenide nanocrystals are not sufficiently understood. In the limited published work on  $\text{MEE}'$  systems, the reason for the formation of a certain crystal phase and shape, when in some cases the thermodynamically unstable cubic phase is formed even at high temperature, is still under debate. Therefore, more research on such alloyed systems is needed, especially on the effect of solvent on their optical properties, composition, and crystal structure.

This work aims at understanding the effect of solvents on the optical properties, crystal phase, shape, and composition of  $\text{CdSe}_x\text{S}_y$  nanocrystals prepared at temperatures between 230 and 300 °C. The solvents used in this study ranged from coordinating to noncoordinating solvents. A feasible relationship between the crystal phase preference (hexagonal or cubic) and the solvent type is described. The nanocrystals were characterized by <sup>31</sup>P and <sup>1</sup>H NMR, UV–vis and attenuated total reflection-IR (ATR-IR) spectroscopies, and other techniques such as energy-dispersive spectrometry (EDS), transmission electron microscopy (TEM), and X-ray diffraction (XRD).

## Experimental Methods

Materials and nanocrystal purification and technical details can be found in the Supporting Information.

- (13) Reiss, P.; Bleuse, J.; Pron, A. *Nano Lett.* **2002**, *2*, 781.
- (14) Peng, X.; Schlamp, M. C.; Kadavanich, A. V.; Alivisatos, A. P. *J. Am. Chem. Soc.* **1997**, *119*, 7019.
- (15) Mekis, I.; Talapin, D. V.; Kornowski, A.; Haase, M.; Weller, H. *J. Phys. Chem. B* **2003**, *107*, 7454.
- (16) Malik, M. A.; O'Brien, P.; Revaprasadu, N. *Chem. Mater.* **2002**, *14*, 2004.
- (17) Qian, H.; Qiu, X.; Li, L.; Ren, J. *J. Phys. Chem. B* **2006**, *110*, 9034.
- (18) Jang, E.; Jun, S.; Pu, L. *Chem. Commun.* **2003**, 2964.
- (19) Swafford, L. A.; Weigand, L. A.; Bowers, M. J.; McBride, J. R.; Rapaport, J. L.; Watt, T. L.; Dixit, S. K.; Feldman, L. C.; Rosenthal, S. J. *J. Am. Chem. Soc.* **2006**, *128*, 12299.
- (20) Bailey, R. E.; Nie, S. *J. Am. Chem. Soc.* **2003**, *125*, 7100.
- (21) Interaction between TOPS and OLA in solution is evident when the two compounds are mixed, leading to a color change to orange, especially with heating, and a 2 ppm chemical shift in phosphorous NMR as compared with pure TOPS.
- (22) Wuister, S. F.; de Mello Donegá, C.; Meijerink, A. *J. Phys. Chem. B* **2004**, *108*, 17393.
- (23) Bryant, G. W.; Jaskolski, W. *J. Phys. Chem. B* **2005**, *109*, 19650.
- (24) Peng, X.; Wickham, J.; Alivisatos, A. P. *J. Am. Chem. Soc.* **1998**, *120*, 5343.
- (25) Kalyuzhny, G.; Murray, R. W. *J. Phys. Chem. B* **2005**, *109*, 7012.

**Cadmium Oleate Precursor.** Cadmium acetate dihydrate (5.33 g, 20 mmol) and oleic acid (22.6 g, 80 mmol) were heated to 150 °C under 20 mmHg vacuum on a rotary evaporator for 2 h. The so-formed liquid was cooled under nitrogen gas, and then dry toluene was added to make a stock solution having a concentration of 0.4 mmol  $\text{g}^{-1}$  in Cd.

**General Method for Nanocrystal Synthesis in Different Solvents.** A cadmium stock solution containing 0.4 mmol of Cd and 8 g of the chosen solvent was charged into a three-neck flask and heated to about 140 °C under vacuum for 1 h to distill off volatiles. Argon gas was admitted, and the mixture was stirred and heated to 300 °C (or to 230 °C when pure oleylamine (OLA), hexadecylamine (HDA), and dioctylamine (DOA) solvents were used). A freshly prepared mixture of trioctylphosphine selenide (TOPSe) and trioctylphosphine sulfide (TOPS) formed by dissolving selenium (0.05–0.5 mmol) and sulfur (2–5 mmol) in 2  $\text{cm}^3$  of trioctylphosphine (TOP) and 0.25  $\text{cm}^3$  of toluene was rapidly injected into the cadmium solution. After injection, the temperature was maintained at 280 °C for crystal growth (except for amine solvents where the temperature was maintained at 230 °C). When the right absorption band edge was reached, the heat was removed and the solution was cooled quickly. Note: The results in Table 1, Figure 3, Figure 4A, Figure 6A, and Figure S5 (Supporting Information) are for nanocrystals prepared in trioctylphosphine oxide (TOPO) using TOP reagent supplied by ICN Pharmaceutical, Ltd. All other data and results are for the nanocrystals prepared in different solvents using TOP reagent obtained from Alfa Aesar. The impurities in TOP can affect the  $\text{CdSeS}$  properties. For the <sup>31</sup>P NMR spectra of these reagents, see the Supporting Information, Figure S1.

### Synthesis in Triphenylphosphine (TPP) without Using TOP.

The cadmium precursor solution (0.4 mmol) was dissolved in triphenylphosphine (8 g) and heated at 120 °C under vacuum for 1 h after which the mixture was heated to 300 °C under an Ar flow. Selenium (0.0063 g, 0.08 mmol) and sulfur (0.0384 g, 1.2 mmol), dissolved in 1-octadecene (ODE) (2  $\text{cm}^3$ ) at 200 °C and cooled to 70 °C, was rapidly injected into the cadmium solution. The crystal growth was carried out at 280 °C.

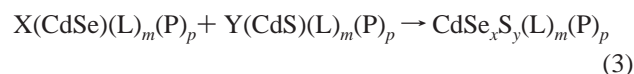
## Results and Discussion

**Nanocrystal Synthesis.** The synthesis of  $\text{CdSe}_x\text{S}_y$  nanoparticles ( $0.04 < x < 0.86$ ,  $0.14 < y < 0.86$ ;  $x + y \approx 0.95 \pm 0.05$ ) was carried out by a single injection of a premixed TOPSe/TOPS precursor into cadmium oleate solutions in TOPO, TOP, TPP, trioctylamine (TOA), and ODE solvents heated at 300 °C and in OLA, HDA, and DOA solvents heated at 230 °C. Cadmium oleate and stearate were found to decompose above 240 °C in the primary and secondary amines OLA, HDA, and DOA. This was caused by the stripping off of the oleate ligands and destabilization of the cadmium ion, which led to the precipitation of cadmium oxide, some of which was further reduced to cadmium metal as evidenced from the XRD pattern of the solid formed as a result of this reaction (see Figure S2, Supporting Information). We attribute this to the reaction of the amine groups of the solvent with the fatty acid anions of the cadmium precursor forming the corresponding amide as confirmed by <sup>1</sup>H and <sup>13</sup>C NMR measurements. Figure S3 (Supporting Information) shows the <sup>1</sup>H NMR spectra for the reaction at 250 °C between oleic acid and oleylamine reagents and between the cadmium oleate precursor and oleylamine and Figure S4 (Supporting Information) shows the <sup>13</sup>C NMR

spectra for these two reactions. The  $^1\text{H}$  NMR spectrum of the liquid taken from the reaction between cadmium oleate and oleylamine after the filtration of the CdO solid is very similar to the spectrum of the amide formed by reacting oleic acid and oleylamine reagents. It shows a signal at  $\delta$  5.95 ppm due to the amide proton of the dialkylamide,<sup>54</sup> which was also confirmed by deuterium exchange, along with the disappearance of the amine proton signal at  $\delta$  1 ppm, which confirms the formation of dioleylamide. CdO also formed when the Cd precursors were heated in 1:3 mixtures of oleylamine dissolved in ODE or in TOA solvents, but it was not observed in 1:3 mixtures of OLA or HDA and TOPO at 300 °C, which may be due to the TOPO–Cd bond being strong enough to stabilize the Cd ion.

In the present study, excess total chalcogen relative to cadmium was used, with added sulfur to Cd and selenium to Cd mole ratios of 2–5 times and 0.05–0.5 times, respectively. Therefore, Se and S precursors compete over the limited amount of Cd ions. Three reactions are expected to take place, as illustrated in Scheme 1.

**Scheme 1.** Steps of the Formation of CdSeS Nanocrystals from Cadmium(II) and Sulfur and Selenium Precursors



where L = oleic acid and/or solvent, P = TOP, TOPS, or TOPSe, and  $k_1$  and  $k_2$  = rate constants of reactions 1 and 2, respectively. Reaction 1 is between Cd oleate and TOPSe to form (CdSe) nuclei, and reaction 2 is between Cd oleate and TOPS to form (CdS) nuclei, with reaction rate constants  $k_1$  and  $k_2$ , respectively. Reaction 3 is the crystal growth to form  $\text{CdSe}_x\text{S}_y$  nanocrystals; however, it is less well defined. It has been reported that the reaction between cadmium oleate and tributylphosphine selenide or sulfide involves the association of two or more molecules to form a transition state where the chalcogen precursor first coordinates to Cd(II) before it undergoes cleavage to form CdSe or CdS;<sup>36d</sup> therefore,  $k_1$  and  $k_2$  are likely to be second or greater order rate constants. It is reasonable to think that reactions 1–3 depend on factors such as the reaction temperature, the type of precursors and their concentrations, cosolvent, and solvent. In this study, the chalcogen precursors' concentration and the solvents were changed. After injection of the chalcogen precursor, oleic acid, solvent, cosolvent, and chalcogen compete for coordination to the nuclei. The solvents used in this study can be classified into coordinating, weakly coordinating, and noncoordinating solvents. ODE is a noncoordinating solvent, while the other solvents contain coordinating groups with different donation power. Some of these ligands are potential metal-site-coordinating ligands, such as TOPO and oleic acid (via oxygen) and amines (via nitrogen) and TOPS (via the S atom) and some are potential chalcogen-site-coordinating ligands, e.g., TOP and TPP (via the P atom) and primary and secondary amines (via weak hydrogen bonding). Therefore, primary and secondary amines can be considered as potential ligands for both the metal and chalcogen sites. All these ligands could play an important role in the nanocrystal growth depending on how strongly they bind to the nanocrystal surface. The oleic acid ligand has been reported to increase the growth rate of CdSe QDs as the number of nuclei formed after injecting TOPSe into cadmium oleate in ODE decreased with increasing oleic acid concentration but remained constant following the initial nucleation step.<sup>48–50</sup> Therefore, in this study, the oleic acid concentration was kept constant and limited to 4 times the Cd ion concentration. In the following sections, we will discuss the effect of the solvents and the added Se/S molar ratio on the properties of CdSeS nanocrystals.

**Composition of the Nanocrystals.** To study the effect of solvents on reactions 1–3 and on the composition of CdSeS nanocrystals, reactions were done using fixed TOPSe and TOPS mole ratios of 0.12 and 3 (corresponding to Se/S of 1:25) relative to cadmium, respectively. These reactant ratios were chosen because they were found to cause a reasonable change in the emission spectra between 500 and 600 nm for all the solvents used. When a Se/S mole ratio higher than

- (26) Peng, Z. A.; Peng, X. *J. Am. Chem. Soc.* **2001**, *123*, 1389.
- (27) Peng, Z. A.; Peng, X. *J. Am. Chem. Soc.* **2002**, *124*, 3343.
- (28) Peng, X. *Adv. Mater.* **2003**, *15*, 459.
- (29) Grebinski, J. W.; Hull, K. L.; Zhang, J.; Kosel, T. H.; Kuno, M. *Chem. Mater.* **2004**, *16*, 5260.
- (30) (a) Jun, Y.-W.; Lee, S.-M.; Kang, N.-J.; Cheon, J. *J. Am. Chem. Soc.* **2001**, *123*, 5150. (b) Joo, J.; Na, H. B.; Yu, T.; Yu, J. H.; Kim, Y. W.; Wu, F.; Zhang, J. Z.; Hyeon, T. *J. Am. Chem. Soc.* **2003**, *125*, 11100.
- (31) Gao, F.; Lu, Q.; Xie, S.; Zhao, D. *Adv. Mater.* **2002**, *14*, 1537.
- (32) Yang, J.; Xue, C.; Yu, S.-H.; Zeng, J.-H.; Qian, Y.-T. *Angew. Chem., Int. Ed.* **2002**, *41*, 4595.
- (33) Peng, X.; Manna, L.; Yang, W.; Wickham, J.; Scher, E.; Kadavanich, A.; Alivisatos, A. P. *Nature* **2000**, *404*, 59.
- (34) Cozzoli, P. D.; Manna, L.; Curri, M. L.; Kudera, S.; Giannini, C.; Striccoli, M.; Agostiano, A. *Chem. Mater.* **2005**, *17*, 1296.
- (35) Meulenberg, R. W.; Strouse, G. F. *J. Phys. Chem. B* **2006**, *110*, 7438.
- (36) (a) Foos, E. E.; Wilkinson, J.; Mäkinen, A. J.; Watkins, N. J.; Kafafi, Z. H.; Long, J. P. *Chem. Mater.* **2006**, *18*, 2886. (b) Becerra, L. R.; Murray, C. B.; Griffin, R. G.; Bawendi, M. G. *J. Chem. Phys.* **1994**, *100*, 3297. (c) Kuno, M.; Lee, J. K.; Dabbousi, B. O.; Mikulec, F. V.; Bawendi, M. G. *J. Chem. Phys.* **1997**, *106*, 9869. (d) Liu, H.; Owen, J. S.; Alivisatos, A. P. *J. Am. Chem. Soc.* **2007**, *129*, 305. (e) Cogne, A.; Grand, A.; Laugier, J.; Robert, J. B.; Wiesenfeld, L. *J. Am. Chem. Soc.* **1980**, *102*, 2238.
- (37) Li, J. J.; Wang, Y. A.; Guo, W.; Keay, J. C.; Mishima, T. D.; Johnson, M. B.; Peng, X. *J. Am. Chem. Soc.* **2003**, *125*, 12567.
- (38) Murray, C. B.; Norris, D. J.; Bawendi, M. G. *J. Am. Chem. Soc.* **1993**, *115*, 8706.
- (39) Yu, K.; Zaman, B.; Singh, S.; Wang, D.; Ripmeester, J. A. *Chem. Mater.* **2005**, *17*, 2552.
- (40) Warner, J. H.; Tilley, R. D. *Adv. Mater.* **2005**, *17*, 2997.
- (41) Talapin, D. V.; Rogach, A. L.; Mekisa, I.; Haubold, S.; Kornowski, A.; Haase, M.; Weller, H. *Colloids Surf., A* **2002**, *202*, 145.
- (42) (a) Pan, D.; Wang, Q.; Jiang, S.; Ji, X.; An, L. *Adv. Mater.* **2005**, *17*, 176. (b) Christian, P.; O'Brien, P. *Chem. Commun.* **2005**, 2817.
- (43) Steigerwald, M. L.; Brus, L. E. *Acc. Chem. Res.* **1990**, *23*, 183.
- (44) Deng, Z.; Cao, L.; Tang, F.; Zou, B. *J. Phys. Chem. B* **2005**, *109*, 16671.
- (45) Sapra, S.; Rogach, A. L.; Feldmann, J. *J. Mater. Chem.* **2006**, *33*, 3391.
- (46) Qu, L.; Peng, Z. A.; Peng, X. *Nano Lett.* **2001**, *1*, 333.
- (47) Cho, K.-S.; Talapin, D. V.; Gaschler, W.; Murray, C. B. *J. Am. Chem. Soc.* **2005**, *127*, 7140.
- (48) Bullen, C. R.; Mulvaney, P. *Nano Lett.* **2004**, *4*, 2303.
- (49) Yu, W. W.; Qu, L.; Guo, W.; Peng, X. *Chem. Mater.* **2003**, *15*, 2854.
- (50) Shukla, N.; Liu, C.; Jones, P. M.; Weller, D. *J. Magn. Mag. Mater.* **2003**, *266*, 178.
- (51) Streckert, H. H.; Ellis, A. B. *J. Phys. Chem.* **1982**, *86*, 4921.
- (52) Yu, W. W.; Wang, Y. A.; Peng, X. *Chem. Mater.* **2003**, *15*, 4300.
- (53) Fedorov, V. A.; Ganshin, V. A.; Korkishko, Y. N. *Phys. Status Solidi A* **1991**, *126*, K5.
- (54) Vandevoorde, S.; Jonsson, K.-O.; Fowler, C. J.; Lambert, D. M. *J. Med. Chem.* **2003**, *46*, 1440.



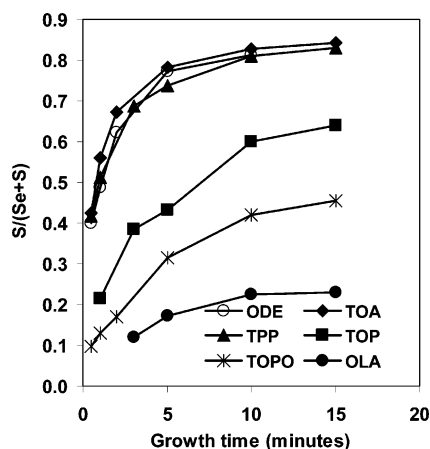


**Figure 1.** Sulfur mole fraction of CdSeS nanocrystals during growth time in different solvents prepared by using a Cd/Se/S reaction mole ratio of 1:0.12:3.

these was employed in primary amine solvents, for example, the change with time in the position of the absorption and emission bands of CdSeS was very small. Figure 1 shows the change with time of the sulfur mole fraction in the nanocrystals obtained from the studied solvents as measured by EDS. The general trend of these plots is that at the initial stage of the reactions, the nanocrystals contain more selenium than sulfur, then the S content builds up during crystal growth, and eventually the plots almost reach a plateau. This indicates that TOPSe reacted with Cd(II) faster than TOPS (i.e.,  $k_1 > k_2$ ) when a premixed TOPSe/TOPS solution was injected, forming Se-rich core nanoparticles, although TOPS was in excess. This is consistent with the literature finding that TOPSe reacts with cadmium oleate faster than TOPS does, when these precursors were used in separate reactions.<sup>36d</sup> It has also been reported that sulfur binds strongly to tributylphosphine so as to inhibit CdS nucleation and growth.<sup>19</sup>

In Figure 1, the change in sulfur mole fraction of the nanocrystals prepared in ODE, TOA, and TPP followed almost a similar path where it sharply increased in the first 5 min then leveled up, while in solvents such as TOPO, TOP, and OLA the S mole fraction increased at a slower rate. When the chalcogen content of the nanocrystals prepared in different solvents is compared after 5 min of reaction time, the Se mole fraction of the nanocrystals as calculated from the inductively coupled plasma (ICP) analysis follows this trend: OLA (0.85) > TOPO (0.67) > TOP (0.55) > TPP (0.28) > ODE (0.24)  $\approx$  TOA (0.23). This series may reflect the trend of  $k_1$  being higher than  $k_2$  in these solvents. The slowest change in sulfur buildup in the nanocrystals and thus the lowest  $k_2$  value took place in OLA solvent, which could be explained by the higher stabilization of TOPS by OLA relative to the other solvents used.<sup>21</sup> The higher S mole fraction found in nanocrystals prepared in TPP as compared with TOP is probably due to the lower stability of TOPS in TPP.

The effect of changing the Se/S mole ratio on the nanocrystal composition was also studied. EDS and ICP analyses on the blue-, green-, yellow-, red- and maroon-emitting QDs prepared in TOPO and using a TOPSe/TOPS precursor that contained different mole ratio of Se/S are given

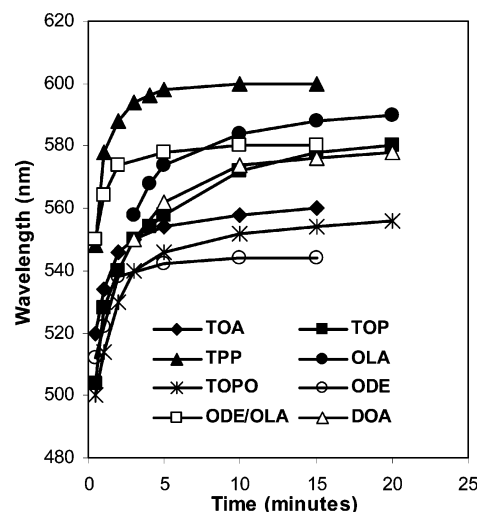


**Figure 2.** Absorption band position of CdSeS nanocrystals prepared using a Cd/Se/S reaction mole ratio of 1:0.12:3 during growth time in different solvents.

**Table 1. Effect of Changing Se/S Reactant Ratio on the Composition of CdSeS Nanocrystals Prepared in TOPO and Isolated after 30 min Reaction Time. Values from EDS and ICP Analyses Are Expressed in Mole Ratios for Samples of (a) Blue QDs; (b) Green QDs; (c) Yellow QDs; and (d) Red QDs**

sample	Se/S added	Se/S in QDs (EDS)	Se/S in QDs (ICP)	composition Cd/Se/S (ICP)
a	1:98	1:17.42	1:18.72	1:0.047:0.88
b	1:18.4	1:4.5	1:4.7	1:0.164:0.77
c	1:3.5	1:2.28	1:2.24	1:0.28:0.628
d	1:1.9	1:1.75	1:1.76	1:0.346:0.61

in Table 1. The Cd/Se/S mole ratio in the purified QDs is not the same ratio used in the reaction mixtures, although they reflect a similar trend. Results clearly indicate that the Se content of the QDs increased on going from the blue- to the red-emitting QDs, while the S content decreased in this series but then almost leveled up beyond the yellow-emitting QDs. We believe that the Se and S composition represents a gradient rather than CdSe core and CdS shell (see XRD results), which agrees with the literature conclusion.<sup>18,19</sup>

**Optical Properties of the Nanocrystals.** The wavelength of the absorption band is a measure of the band gap of the nanocrystals. The band gap for bulk  $\text{CdSe}_x\text{S}_y$  is between that of CdSe (1.7 eV)<sup>22</sup> and CdS (2.5 eV)<sup>23</sup> and changes linearly with the composition.<sup>53</sup> In a given solvent, when the Se/S mole ratio was changed, the absorption and emission of the nanocrystals also changed; therefore, in order to assess the solvent effect on the optical behavior of the CdSeS nanocrystals, a fixed Cd/Se/S mole ratio of 1:0.12:3 was used and the spectra were measured with respect to time (Figure 2). This ratio was chosen to cause a reasonable shift in the absorption and emission bands of the nanocrystals in different solvents between 500 and 600 nm (see discussions above). In general, these plots show a quick shift of the absorption bands to the red region within the first 5 min of reaction then a slowing to an almost constant wavelength. However, when TOPSe/TOPS precursor was injected into Cd/oleate/OLA or DOA solutions, the solution color (and spectrum above 400 nm) did not change immediately, and only after a 2 min delay was a sudden change in the solution color observed with an excitonic peak at 558 nm. The delay might

be due to the stabilization of the chalcogen precursors and/or the first formed nuclei by these amines via hydrogen bonding.<sup>21</sup>

Although the profile of plots in Figures 1 and 2 are similar, careful inspection shows that the trends are different. In Figure 2, the shift in absorption band reflects not only the change in the sulfur mole fraction but also the effect of solvents on the size of the nanocrystals. Under the reaction conditions, the fastest red shift in the absorption band of CdSeS nanocrystals was for the reaction in TPP and the slowest absorption shift was recorded for the TOPO solvent. Although TPP is one of the solvents that led to nanocrystals with highest S and lowest Se mole fractions (see above), the fastest red shift in the absorption band is more likely due to the fast growth of the particles in this solvent. In fact, after 5 min of reaction, the nanoparticles obtained from TPP had an average size of 9 nm as compared with 3.5 nm obtained in TOPO. This may be explained by the TPP molecule being small and more labile and, therefore, is less effective in slowing down the nanocrystals growth when compared with the long-chain TOPO and TOP molecules, which were reported to slow down the crystal growth.<sup>9b</sup> The delocalization of the lone pair of the phosphorus atom of TPP over the three phenyl rings of the molecule could make it a weaker ligand and therefore more labile than the TOP ligand. The difference is obvious from the phosphorus chemical shifts of TPP ( $\delta$  -4 ppm) and TOP ( $\delta$  -29.7 ppm) (see Table S2, Supporting Information).

When 30 wt % of OLA or HDA cosolvents were used with TOPO, the excitonic band position of CdSeS could be shifted to as high as 630 nm using a Se/S mole ratio of 0.5:2 accompanied by a narrow distribution of particle size as indicated by TEM. The HDA cosolvent in TOPO has been reported to slow down the crystal growth of CdSe nanocrystals compared with pure TOPO solvent accompanied by fast focusing of the size distribution.<sup>12,36a</sup> Therefore, this bigger shift in band position is due more to an enrichment of the nanocrystals with Se, as indicated by EDS elemental analysis, than to an increase in the particle size. Similarly, when primary amines were added as cosolvents with TOA or ODE, we also found that the red shift of the absorption band became faster.

The QY of the emission band of the nanocrystals was enhanced by selecting appropriate amounts of selenium and sulfur precursors. For example, nanocrystals of high QY in the blue region were prepared by using a smaller ratio of selenium to sulfur in the synthesis, ca. 0.05 mmol of Se and 5 mmol of S, and for the synthesis of high-QY red-emitting nanocrystals, more selenium and less sulfur were used, ca. 0.5 and 2 mmol, respectively. A QY of up to about 0.8 was obtained for CdSeS nanocrystals prepared in TOPO, TOA, and ODE, while in other solvents, the QY ranged between 0.3 and 0.5. The high QY could be attributed to the high content of CdS (inorganic passivation), but ligand passivation could not be ruled out. The effect of ligands on the QY, especially in TOPO, is being investigated in our laboratory.

Figure 3 shows how the wavelength of emission peaks in TOPO shifted when different Se/S mole ratios were used. The emission bands are narrow with full width at half-

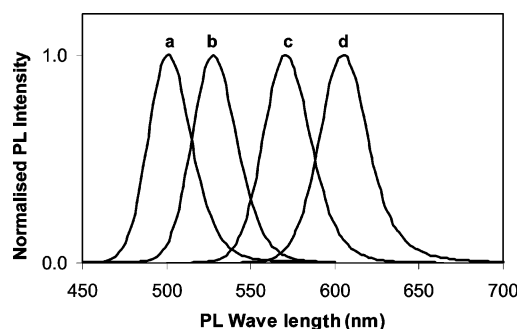


**Figure 3.** PL spectra of CdSeS nanocrystals prepared in TOPO using different reactant Se/S mole ratios as in Table 1. (a) Blue QDs (Se/S = 1:98); (b) green QDs (Se/S = 1:18.4); (c) yellow QDs (Se/S = 1:3.5); (d) red QDs (Se/S = 1:1.9).

maximum (fwhm) of 29 nm but become broader for the red-emitting QDs when pure TOPO is used, which was improved by the use of either OLA or HDA as cosolvents with TOPO (fwhm of 29 nm), as an indication of narrow particle size distribution.<sup>2b,24</sup> The effect of adding HDA cosolvent to TOPO on the purity of the emission spectra of CdSeS nanocrystals is illustrated in Figure S5 (Supporting Information), which shows that the emission band became narrower and symmetrical when the mixed solvent TOPO/HDA was used. In most of the preparations, usually the highest QY at a certain Se/S ratio was achieved within the first 5–10 min of reaction, where at this time the sulfur mole fraction approached a plateau. The CdSe to CdS lattice mismatch is only 3.9%, which should produce high-quality nanocrystals with a few defects resulting in high QY.<sup>11,14</sup> Nanocrystals prepared in primary and secondary amines showed only a moderate QY of ~0.3–0.4 compared with those synthesized in the other solvents, which may be due to enrichment of the nanocrystals with Se and having less sulfur (e.g., Se/(Se + S) > 0.77), which could result in some surface defects.<sup>15</sup> We have noticed that the QY and solubility of the amine-functionalized nanocrystals were reduced after several steps of purification due to the loss of the amine capping ligands during washing that could have led to insufficient passivation of the surface traps and reversed their effect on PL.<sup>12,25</sup>

**Shape and Size of the Nanocrystals.** TEM measurements showed that different solvents have different effects on the size and shape of the nanocrystals at a given time of reaction (see Supporting Information, Table S1 and Figures S6–S13). TEM measurements showed that most of the nanocrystals prepared in solvents such as TOPO, TPP, DOA, TOA, and ODE or these solvents mixed with the cosolvent OLA or HDA have a spherical shape. When the reaction was left for longer than 30 min, anisotropic nanocrystals formed; e.g., in TOPO, oval nanocrystals developed as shown in Figure 4A. Usually, the PL color of spherical CdSe nanocrystals prepared in TOPO can be tuned by changing the QD size from ca. 2 to 8 nm;<sup>9a,12,49</sup> however, in this study the CdSeS QDs of different PL colors, prepared in TOPO solvent using different Se/S mole ratios, exhibited a narrower size range of 2.5–4.5 nm. The PL of nanocrystals prepared in TOA can be tuned from blue to red color with an average size ranging between 4 and 8 nm by changing the Se/S mole ratio.

Reactions in OLA and TOP produced spherical nanocrystals at the initial stage of the reaction, but after 5 min

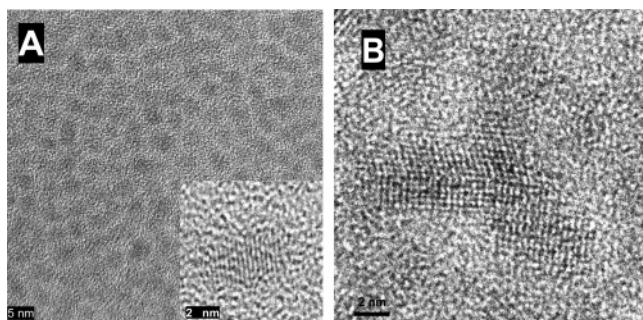


**Figure 4.** (A) TEM image of yellow-emitting CdSeS QDs prepared in TOPO after a 45 min reaction time at 300 °C (scale bar = 5 nm); the inset is a HRTEM image of an oval QD (scale bar = 2 nm). (B) HRTEM image of a tripodal red-emitting nanocrystal prepared in OLA at 230 °C after a 20 min reaction time (scale bar = 2 nm).

elongated crystals were detected, and at 20 min some other shapes such as nanorods and tripodal nanocrystals formed, as in Figures 4B, S7, and S13 (Supporting Information). The length of these nanorods and tripods increased with reaction time, while the width was maintained at around 3.5 nm. Size and shape control of nanocrystals has been previously reported for CdSe<sup>26–29</sup> and CdS<sup>30–33</sup> nanocrystals, but not for CdSeS nanocrystals. CdSe nanocrystals of different anisotropic shapes can form in TOPO or ODE at 300 °C by increasing the Cd concentration from 0.067 to 0.433 mol kg<sup>−1</sup> to give short rods, long rods, and then branched crystals.<sup>26,27</sup> This was attributed to the presence of magic-sized nanoclusters that acted as seeds for the anisotropically shaped nanocrystals with a short axis close to 3 nm in length. It has been reported that when CdS and ZnSe were prepared in HDA, the amine surfactant increased the growth rate in the (001) direction leading to rod or branched nanocrystals, respectively.<sup>30,34</sup> In all of our syntheses, we used a relatively low cadmium concentration of ~0.047 mol kg<sup>−1</sup>, yet in some solvents, such as TOP and OLA, elongated shapes were obtained. We attribute the growth along a certain axis of nanocrystals prepared in these solvents to a solvent effect where chalcogen-site-stabilizing solvents are used. However, spherical CdSeS nanocrystals of different sizes were obtained in 1:3 mixtures of OLA/TOPO or OLA/ODE similar to CdSe nanocrystals reported in a HDA/TOPO mixture.<sup>12</sup>

**ATR-IR Spectra.** The ATR-IR spectra of QDs prepared in TOA, DOA, ODE, and TPP showed an absorption band at 1533–1537 cm<sup>−1</sup> (see Supporting Information, Figure S14A) which is due to the (COO) asymmetrical stretching of the oleate ligand capped onto the surface of the nanocrystals, indicating the presence of bidentate carboxylate bonding.<sup>50</sup> The IR spectra of the QDs prepared in TOA and TPP exhibited weak absorption bands around 1020 cm<sup>−1</sup> due to the P=O stretching in TOPO or TPPO.<sup>1c,34</sup> These phosphine oxides can form by the oxidation of TOP or TPP in air during the nanocrystal separation and purification. However, the IR spectra of the purified QDs prepared in DOA and ODE did not show the P=O absorption band of TOPO. This may indicate that the nanocrystals prepared in these two solvents were capped with the oleate ligand.

The IR spectra of the CdSeS nanocrystals prepared in TOPO and TOP solvents showed strong and broad absorption bands centered at 1020–1080 cm<sup>−1</sup> due to P=O stretching

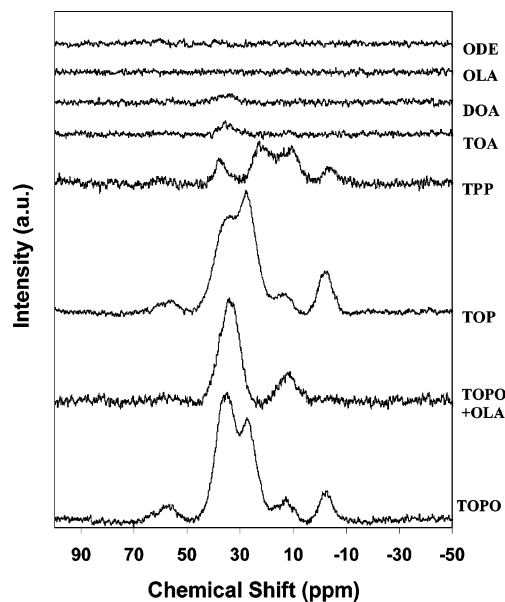


**Figure 5.** <sup>31</sup>P NMR spectra of the CdSeS nanocrystals prepared in different solvents.

of the TOPO ligand capped on the nanocrystals, but such a band was not observed in the spectrum of nanocrystals prepared in OLA (see Supporting Information, Figure S14B). Absorption that is due to the (COO) asymmetrical stretching of the oleate ligand was not observed for the nanocrystals prepared in TOPO, indicating that these nanocrystals are mainly capped with TOPO, but a very weak band at 1556 cm<sup>−1</sup> appeared in the spectrum of QDs prepared in TOP. On the other hand, a medium intensity band at 1547 cm<sup>−1</sup> due to (COO) asymmetrical stretching was observed for those QDs prepared in OLA. The IR spectrum of nanocrystals prepared in OLA also showed a weak absorption at 3250 cm<sup>−1</sup> which could be attributed to the (NH) stretching.<sup>35</sup> However, the (NH<sub>2</sub>) scissoring was not observed, and it could be masked by the carboxylate group band. A very weak absorption at about 1645–1707 cm<sup>−1</sup> observed in the spectra of nanocrystals prepared in TOPO and TOP could be attributed to free oleic acid contamination. Neat oleic acid shows strong C=O stretching absorption at 1707 cm<sup>−1</sup>.

**NMR Spectra.** Very few <sup>31</sup>P NMR studies on CdSe nanocrystals prepared in TOPO/TOP solvent have been reported.<sup>36a–d</sup> The <sup>31</sup>P NMR spectra of the CdSeS QDs prepared in different solvents, as illustrated in Figure 5, show very interesting features depending on the solvent used in the synthesis (see Supporting Information, Table S2, for <sup>31</sup>P and <sup>1</sup>H NMR data). In general, the phosphorus NMR spectra of the nanocrystals taken after two rounds of washing showed two types of phosphorus signals, sharp and broad. The sharp signals are due to the presence of free phosphorus species in solution, which usually disappeared after a few more washings and centrifugation. The broad peaks, which persist after washing, are due to surface-tagged phosphorus species.<sup>36b,c</sup> The large diameter of these nanocrystals may arrest their tumbling motion in solution leading to incomplete averaging, which results in the broadness of these signals.

Two sharp signals were observed at chemical shifts (δ) 49.9 and 49.7 ppm at 30 °C in the <sup>31</sup>P NMR spectrum of CdSeS QDs prepared in TOPO and washed twice. These



are very close to the  $\delta$  values of 48.6 and 48.5 ppm reported recently for TOPS and TOPO, respectively.<sup>36d</sup>  $^{31}\text{P}$  NMR measurements on the QD solutions at variable temperatures ranging from +40 °C to -20 °C showed that by lowering the temperature, the first signal remained almost stationary while the second signal moved to a lower field (see Supporting Information, Figure S15). This behavior was found to be very similar to the behavior of a mixture of TOPS and TOPO reagents in  $\text{CDCl}_3$ ; therefore, these sharp signals are assigned to free TOPS and TOPO in the solution. A signal for free TOPSe could not be detected, which may indicate that most of this selenium precursor had reacted. TOPSe itself showed a signal at 37.5 ppm with two satellites ( $J_{\text{P-Se}}$  spin splitting of 680 Hz), which are within the previously reported values of 37.5 ppm and 650–684 Hz, respectively, for  $\text{R}_3\text{P=Se}$  in  $\text{CDCl}_3$ .<sup>36d,e</sup>

Also, two intense and three weaker broad  $^{31}\text{P}$  signals were recorded for the QDs prepared in TOPO and are assigned to surface-coordinated phosphorus species (see Figure 5). The two intense broad bands at  $\sim 34$  and  $\sim 26.6$  ppm, which are very close to the literature values of 20–34 ppm,<sup>36c</sup> may be respectively assigned to TOPS and TOPO coordinating to Cd sites at the nanocrystal surface. These two bands appeared at higher fields (shielded rather than deshielded) than those for free TOPS and TOPO, which could be due to the shielding effect of the large size nanocrystals as compared with the phosphorus ligand.<sup>36b</sup> In fact, a weaker broad band downfield from the chemical shift of the free phosphorus species was recorded at 56 ppm, which could also be assigned to surface TOPS or TOPO.<sup>36c</sup> Furthermore, when TOPO/TOP-tagged QD solution was shaken with excess mercaptopropionic acid (MPA) at room temperature, the broad band at 25 ppm disappeared, which could be indicative of the replacement of the TOPO ligand with the MPA ligand. It is known that the TOPO ligand can be easily replaced by the MPA ligand.<sup>5</sup> However, the band at 34 ppm, which is assigned to surface TOPS and the other weak bands, disappeared only when this solution was heated. This reaction resulted in the appearance of sharp phosphorus peaks due to free phosphorus species in the  $^{31}\text{P}$  NMR spectrum of the mixture, presumably as a result of ligand exchange. Other weak broad bands at 11.5 and -3 ppm ( $\Delta\delta = 14.5$  ppm) may be assigned to TOP species coordinating to S and Se sites ( $\text{TOP} \rightarrow \text{S}$  and  $\text{TOP} \rightarrow \text{Se}$ ) at the surface of the nanocrystals, respectively. This assignment is based on two facts, the first one that the signal for free TOP with a  $\text{P}^{3+}$  atom occurs at a higher field ( $\delta -29.7$  ppm) than those for TOPS and TOPSe (49.9 and 37.5 ppm, respectively), which both have the  $\text{P}^{5+}$  atom. This order of chemical shift occurrence is also expected to happen if these three species are tagged to the surface of the nanocrystals, where  $\text{TOP} \rightarrow \text{S}$  and  $\text{TOP} \rightarrow \text{Se}$  signals were essentially observed at higher field than those for the TOPS and TOPSe signals. Second, the difference between the  $^{31}\text{P}$  NMR signal for the free species TOPS and TOPSe is  $\Delta\delta = 12.4$  ppm, which is very close to the difference between the broad bands at 11.5 and -3 ppm ( $\Delta\delta = 14.5$  ppm) that are assigned to surface  $\text{TOP} \rightarrow \text{S}$  and  $\text{TOP} \rightarrow \text{Se}$  species, respectively. The  $^1\text{H}$  NMR spectra of these nanocrystals showed strong and broad signals

assigned to the protons of alkyl groups of the phosphorus ligands with no apparent signal for the ethylene protons of oleic acid. Nanocrystals with different emission colors that were prepared in TOPO gave very similar  $^{31}\text{P}$  and  $^1\text{H}$  NMR spectra.

The NMR spectrum of QDs prepared in TOP showed both types of sharp signals at 49.8 and 49.6 ppm and broad phosphorus bands at 34, 27.6, 12.5, and -3.3 ppm. The sharp signals disappeared after several washings. These are in positions similar to those prepared in TOPO and therefore are similarly assigned. It is known that commercial TOP contains about 10% TOPO, which we confirmed by  $^{31}\text{P}$  NMR, and extra TOPO could form by the oxidation of TOP solvent during the nanocrystal precipitation process. The  $^1\text{H}$  NMR spectrum did not show a signal for the hydrogen of the alkene group of oleic acid.

The  $^{31}\text{P}$  NMR spectrum of the QDs prepared in TPP and washed twice showed a sharp signal at 30.3 ppm assignable to free TPPO (see Table S2, Supporting Information), which disappeared after a few washings. Also, broad peaks at 37, 10.6, and -3.3 ppm were recorded and can be assigned to TOPS coordinated to Cd sites, TOP coordinated to S sites, and TOP coordinated to Se sites, respectively, as discussed above. Another broad peak at 22.7 ppm was recorded for these nanocrystals, which is probably too far from being assigned to surface TOPO species, but could be assigned to TPPO surface species. To confirm this, the synthesis in TPP was done using Se and S powders dissolved in ODE instead of with TOPSe/TOPS as precursors, where only one weak broad phosphorus band was obtained at 22.5 ppm, which could be only assigned to TPPO bound to cadmium sites. The  $^1\text{H}$  NMR spectrum showed signals due to protons of the ligand alkyl groups and a very weak and broad signal at  $\sim 7.15$  ppm, which could be due to the aromatic protons of TPPO. The spectrum also showed a broad and weak signal at 5.2 ppm, which is assigned to the alkene hydrogen atoms of the oleic acid. Such a signal has been reported to occur at 5.3 ppm in the  $^1\text{H}$  NMR spectrum of oleic acid-capped CdTe nanocrystals.<sup>52</sup> Oleic acid itself exhibits a multiplet signal centered at 5.35 ppm due to the alkene hydrogen atoms.

The  $^{31}\text{P}$  NMR spectra of the QDs prepared in OLA and in ODE did not show any signals due to surface phosphorus species, while the  $^1\text{H}$  NMR spectra revealed weak signals at 5.2 ppm assignable to alkene protons of oleic acid. A weak signal at 1.05 ppm due to  $\text{NH}_2$  protons was observed for the OLA-capped nanocrystals. QDs prepared in a mixture of OLA and TOPO showed two broad peaks at 34 and 12 ppm assignable to surface TOPS coordinated to Cd sites and TOP coordinated to S sites, respectively. The  $^{31}\text{P}$  NMR spectrum of the QDs prepared in DOA showed only a trace of a broad peak at 34 ppm assignable to TOPS coordinated to Cd sites. The  $^{31}\text{P}$  NMR spectrum of the QDs prepared in the tertiary amine, TOA, showed very weak broad peaks at 37 and 12 ppm assignable to surface TOPS coordinated to Cd sites and TOP coordinated to S sites, respectively, and the  $^1\text{H}$  NMR spectrum showed a broad and weak signal assigned to alkene protons of oleic acid at 5.27 ppm.

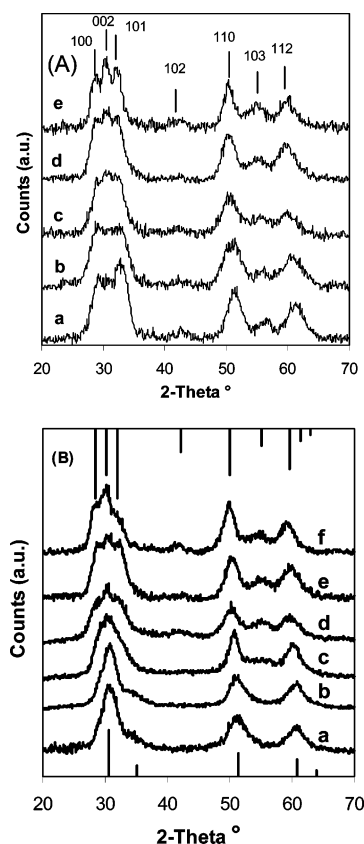


**Figure 6.** XRD patterns for CdSeS nanocrystals prepared in different solvents. (A) XRD patterns for nanocrystals prepared in TOPO using different ratios of Se/S as in Table 1 and that prepared in TOPO/HDA. Key: (a) blue; (b) green; (c) yellow; (d) red; and (e) maroon prepared in TOPO/HDA mixture. (B) XRD patterns for nanocrystals prepared using a Cd/Se/S ratio of 1:0.12:3 in (a) ODE; (b) TOA; (c) TPP; (d) TOP; (e) TOPO; and (f) OLA. The upper and lower bar lines represent typical wurtzite and zinc blende diffraction lines, respectively.

From the phosphorus NMR results, one might conclude that QDs prepared in the coordinating solvents TOPO and TOP are stabilized by some phosphorus species coordinated to Cd, S, and Se sites, and IR and  $^1\text{H}$  NMR measurements demonstrated the absence of oleate ligands. The QDs prepared in TPP are stabilized by the TOP ligand coordinated to the S and Se sites as well as by TOPS, TPPO, and oleic acid. In the primary amine solvent, OLA, the QDs are mainly stabilized by amine and oleate ligands, as evident from IR and  $^1\text{H}$  NMR measurements. In the weakly coordinating solvents, TOA and DOA, the QDs are stabilized mainly by the oleate ligand plus very small amounts of TOP and TOPS. However, in the noncoordinating solvent ODE, the QDs are unambiguously stabilized by the oleate ligand.

**X-ray Diffraction of the Nanocrystals.** The CdSeS nanocrystals could adopt either of the most common phases found in CdSe or CdS, hexagonal or cubic. It is known that the cubic phase of CdSe and CdS is stable at room temperature, but it transforms reversibly to the hexagonal phase above  $95 \pm 5$  °C.<sup>53</sup> Figure 6A illustrates the XRD patterns of the nanocrystals that were prepared using different molar ratios of Se/S in TOPO and that emit in the blue, green, yellow, and red regions of the visible spectrum. All these XRD patterns show diffractions in the planes (100), (002), (101), (102), (110), (103), and (112) that correspond to hexagonal crystal structures. The  $2\theta$  values for all diffraction peaks lie between that of pure CdS and pure CdSe, which

indicates that selenium and sulfur are alloyed in these nanocrystals and that the particles do not consist of separate CdS and CdSe domains.<sup>18,19</sup> There is a slight shift toward lower diffraction angles in all of the diffraction lines when moving from the blue-emitting (a) to the red-emitting (e) nanocrystals. This slight increase in the  $d$  spacing in this series is attributed to the presence of more Se and less S content in the red-emitting crystals as compared with the blue-emitting crystals (see the elemental composition in Table 1).

Another interesting feature in the XRD patterns of these CdSeS materials is the progressive increase in intensity of the (002) diffraction line in moving from the blue- to the red-emitting QDs. This line, which is due to diffraction in the plane perpendicular to the  $c$  axis of the crystals, gains about 30% in intensity relative to the (100) diffraction line in this series. The increase in intensity in this series may be attributed to the increase in the electron density in this crystal plane of a hexagonal structure due to the enrichment of Se in the (002) plane, thus approaching a pattern similar to the pattern of some reported hexagonal CdSe nanocrystals.<sup>2,12,37,46</sup>

QDs that have been prepared using other solvents were found to adopt either a hexagonal or a cubic phase. To understand the solvent effect on the evolution of the crystal phase of the nanocrystals, the syntheses were done in different solvents using a fixed mole ratio of Cd/Se/S of 1:0.12:3. The XRD patterns of some selected measurements are shown in Figure 6B (see also Supporting Information, Table S3, for selected-area electron diffraction (SAED) data). The elongated CdSeS nanocrystals, prepared in TOP at 300 °C and in OLA at 230 °C, have a hexagonal structure, similar to that of CdS nanocrystals and nanorods prepared in primary amine solvents,<sup>30a,40</sup> with a pronounced intensity of diffraction line (002) due to the larger number of planes along the  $c$  axis of the nanocrystals.<sup>38,39</sup> On the other hand, the XRD measurements on the nanocrystals prepared in the secondary amine solvent, DOA, at 230 °C resulted in nanocrystals of a cubic structure;  $2\theta = 31^\circ$  (111),  $51^\circ$  (220), and  $61^\circ$  (311). Similarly, all the nanocrystals prepared in TOA and ODE solvents at 300 °C showed a cubic structure, although this reaction temperature is higher than that used in the OLA and HDA solvents and similar to that used in the TOPO solvent, which produced a hexagonal structure. XRD measurement of the CdSeS QDs prepared in TPP (Figure 6B) showed diffraction lines at  $2\theta = 30.5^\circ$  (111),  $50.7^\circ$  (220), and  $60.2^\circ$  (311) that correspond to a cubic structure, but with a shallow valley between the (220) and (311) diffractions where the hexagonal diffraction line (103) usually appears, whereas diffraction (102) could not be seen. The excessive broadening in the (102) and (103) lines is characteristic of stacking faults.<sup>1d,34,43,52</sup> SAED measurements on these nanocrystals could not indicate a decisive structure; therefore, the structures of these QDs can be regarded as hybrids of cubic and hexagonal phases.

The reason for the high-temperature formation of a cubic phase of CdSeS in some solvents and the formation of a hexagonal phase in other solvents is subject to debate. It is known that the hexagonal wurtzite crystal phase of CdSe or CdS is thermodynamically more stable than the cubic zinc blende phase at elevated temperature,<sup>12,38,53</sup> while the cubic phase is favored at low temperature.<sup>41,42</sup> The evolution of



the hexagonal or cubic phase was reported to depend on the concentration of Cd ion, where hexagonal CdS nanocrystals formed at low Cd concentration (thermodynamic control), while a cubic structure formed at higher concentrations (kinetic control) in hexadecylamine at 140 °C.<sup>42b</sup> The formation of cubic-phase CdSe nanocrystals in a phosphine-free synthesis in paraffin/oleic acid at 200–240 °C was attributed to the lower growth temperature.<sup>44</sup> In a more recent study of a phosphine-free synthesis of CdSe nanocrystals in olive oil/oleic acid at 230–300 °C, the authors attributed the development of the cubic structure to the absence of TOP and TOPSe ligands in the reaction.<sup>45</sup> In our study, TOP, TOPSe, TOPS, and a constant cadmium oleate concentration (47 mmol kg<sup>-1</sup>) were used in all of these high-temperature syntheses, yet we could still obtain either a hexagonal or a cubic structure. Although the reaction temperature, concentration, and the presence or absence of TOP or TOPSe are probably important factors, the effect of solvent seems to have been overlooked in the literature when the crystal structure of such nanoparticles has been discussed. The CdSeS nanocrystals prepared in TOPO and TOP at 300 °C and in HDA and OLA at 230 °C adopted the thermodynamically stable hexagonal phase, while those prepared in TOA and ODE at 300 °C and in DOA at 230 °C exhibited a cubic structure, and a hybrid structure formed in TPP at 300 °C. Here, the evolution of the crystal phase of CdSeS nanocrystals could be rationalized as being solvent dependent rather than concentration or temperature dependent, depends on the coordinating power of the solvent, and therefore depends on the type of surface ligands that stabilize the nanocrystal, as explained below.

**Correlation of the Results.** ATR-IR, <sup>1</sup>H NMR, and <sup>31</sup>P NMR spectroscopy were used to identify the ligands capped on the surface of the nanocrystals prepared in different solvents, while the crystal structures were determined from their XRD patterns. We may correlate these results to identify the important role of solvents in determining the QD shape and structure. We have noticed a coherent relationship between the solvent properties and the crystal phase and shape of the QDs prepared in them. This can be summarized as follows:

*Type A, Coordinating Solvents, Hexagonal Structure.* (1) All QDs prepared in pure TOPO or TOPO/cosolvent and in TOP solvent at 300 °C have a hexagonal structure with abundant TOPO and TOPS surface-capped to Cd sites and some TOP surface-capped to S or Se sites. (2) QDs prepared in the pure primary amine solvents OLA and HDA at 230 °C also have a hexagonal structure with no surface-capped TOPO or TOP molecules, but there is evidence (from IR and NMR) of the presence of amine and oleic acid ligands. Therefore, QDs prepared in Cd-site-coordinating solvents end up having a hexagonal structure. TOP and RNH<sub>2</sub> can be considered as potential ligands to chalcogen sites, and therefore, they may have had some effect on the growth of elongated crystals by activating the crystal surface along the *c* axis.

*Type B, Weak or Noncoordinating Solvents, Cubic Structure.* All QDs prepared in the weakly coordinating solvents TOA and DOA and in the noncoordinating solvent ODE at

300 °C have a cubic structure with very little or no TOPO, TOPS, and TOP coordinated to Cd or chalcogen sites, but the nanocrystal are predominantly surface-capped with oleic acid. Therefore, QDs prepared in weak or noncoordinative solvents end up having a cubic structure.

*Type C, Nonsurfactant Solvents, Distorted Structure.* QDs prepared in TPP have a hybrid crystal structure of hexagonal and cubic phase with some TOPS and TPPO surface-capped to Cd sites and TOP surface-capped to chalcogen sites. Therefore, QDs prepared in a solvent that is not a surfactant end up forming distorted structures intermediate between the hexagonal and cubic phases.

With the available data in this study, we have demonstrated the effect of different solvents on the properties of CdSeS nanocrystals. We envisage that in the coordinating solvents, the abundant solvent molecules can coordinate to Cd(II), stabilize the CdSeS nuclei, slow down the crystal growth, and produce a hexagonal phase. In weak or noncoordinating solvents, the crystal growth is faster and leads to the formation of the cubic phase.

## Conclusion

In this study, CdSeS nanocrystals of medium to high quantum yield emission were prepared using several solvents having different coordination power. We have shown in detail using different characterization techniques that capping ligands on CdSeS nanocrystals depend on the solvent and precursors used in the synthesis. The type of solvent and therefore the capping ligands were shown to play a significant role in developing the crystal phase, composition, size, shape, and optical properties of these nanocrystals. Coordinating solvents such as TOPO, OLA, TOP, etc., can lead to hexagonal-structure nanocrystals while weak or noncoordinating solvents such as TOA, DOA, and ODE can produce a cubic structure even at high temperature. It has also been concluded that nanocrystals prepared in TPP can have a hybrid structure of hexagonal and cubic phases in the same nanocrystals. Some solvents led to the formation of sulfur-rich nanocrystals and others led to the formation of selenium-rich nanocrystals.

**Acknowledgment.** This research was funded by the Foundation for Research, Science and Technology of New Zealand under Contract No. UOOX0403. Thanks go to Professor D. Green and R. Easingwood of the University of Otago, N.Z., for coordinating the resources and doing some of the TEM measurements, respectively. We thank Dr. H. Wong, of Industrial Research, for the NMR measurements and useful discussions.

**Supporting Information Available:** Reagents, experimental and technical details; tables of particle size, NMR data, and XRD and SAED data; <sup>31</sup>P NMR spectra of TOP reagents; XRD pattern of CdO/Cd deposit in OLA solvent; <sup>1</sup>H and <sup>13</sup>C NMR spectra of oleylamide product; visible spectra of QDs prepared in TOPO and TOPO/HDA; TEM images and SAED patterns of CdSeS QDs obtained in different solvents; ATR-IR spectra of QDs; variable-temperature <sup>31</sup>P NMR spectra of CdSeS QDs prepared in TOPO (PDF). This material is available free of charge via the Internet at <http://pubs.acs.org>.

CM070818K